

## Photon-photon correlations in Ag+Ag collisions at $\sqrt{s_{NN}} = 2.55$ GeV

M. GRUNWALD(\*) for the HADES COLLABORATION

*Warsaw University of Technology, Faculty of Physics - Warsaw, Poland*

received 23 July 2024

**Summary.** — The investigation of femtoscopic correlations between pairs of photons emitted from heavy-ion collisions offers a unique opportunity to investigate the evolving source spacetime characteristics and properties. Unlike commonly studied charged particle correlations, photons are not influenced by strong or electromagnetic interactions, and thus have a longer mean free path. These characteristics indicate that the information they carry remains minimally distorted from their point of origin until detection in experiment. Consequently, it becomes feasible to examine source characteristics not solely based on post thermal freeze-out phases, but also encompass earlier stages of the expansion, without significant distortions caused by neighboring particles. However, photon detection presents a non-trivial challenge, necessitating either a specialized approach of reconstructing photons converted into dilepton pairs, or detectors capable of detecting neutral particles. Additionally, the photon yield is vastly dominated by the decay of  $\pi^0$  mesons, happening way after thermal freeze-out. Hence femtoscopy is sensitive to the emission sequence of particles, may offer a plausibility of distinguishing between the femtoscopic signal of direct photons and decay photons. As a constituent of the FAIR/GSI scientific complex, the HADES experiment specializes in detecting light vector mesons through dielectron ( $e^\pm$ ) channels generated during high-energy collisions of heavy ions, typically at energies around several (1-2) A GeV. By utilizing various detectors within the spectrometer, a photon sample can be acquired. The preliminary results from data of Ag+Ag collisions at  $\sqrt{s_{NN}} = 2.55$  GeV, as measured by HADES experiment, will be presented.

### 1. – Introduction

Among many particle species created in heavy-ion collisions, photons exhibit few unique properties. Their immunity to strong and electromagnetic interactions, resulting in a long mean free path, renders them invulnerable to medium effects. Consequently, the information carried by such particles endure from the moment of their emission until detection in experiment. This is particularly advantageous in the context of continuous

(\*) E-mail: [mateusz.grunwald.dokt@pw.edu.pl](mailto:mateusz.grunwald.dokt@pw.edu.pl)

photon emission, in contrast to post kinematic freeze-out emission of most other particles, effectively making photons an ideal probe for investigating early stages of the collision [1].

Unfortunately, photon detection is challenging from an experimental standpoint, often limiting their use in many analysis. Additionally, the vast range of potential photon origins complicates the differentiation between direct photons (created before freeze-out) and decay photons (being a product of particle decays). Moreover, because photon yield is strongly dominated by  $\pi^0$  decay (being almost exclusively  $\pi^0 \rightarrow \gamma\gamma$ ) such differentiation becomes even harder.

## 2. – Femtoscopy

Femtoscopy [2], originating from HBT measurements [3], is a method of exploring space-time properties of the source area. Due to being very small and short-lived ( $R \sim 10^{-15}$  m,  $\tau \sim 10^{-23}$  s) such object cannot be directly probed. Instead, femtoscopy relies on particle correlations in the momentum frame, due to interactions between them and/or effects of quantum statistics. The correlation function can be defined as:

$$(1) \quad CF(q) = \int S(q, \mathbf{r}) |\Psi(q, \mathbf{r})|^2 d\mathbf{r}^3 = \frac{\text{Same}(q)}{\text{Mixed}(q)}$$

where:  $q = |\mathbf{p}_1 - \mathbf{p}_2|$  is the momentum difference,  $S(q, \mathbf{r})$  is the source function,  $\Psi(q, \mathbf{r})$  is the 2-particle wave function,  $\text{Same}(q)/\text{Mixed}(q)$  are the  $q$  distributions from same/mixed events respectively. The same/mixed event approach is used experimentally, since  $S(q, \mathbf{r})$  is inaccessible directly and  $\Psi(q, \mathbf{r})$  is not always known (*i.e.* due to unknown interaction parameters).

In case of identical, non-interacting bosons, emitted from the Gaussian source, the correlation function can be parametrized as:

$$(2) \quad CF(q_{INV}) = 1 + \lambda e^{-q_{INV}^2 R_{INV}^2}$$

where  $R_{INV}$  is the invariant HBT radius,  $\lambda$  is the correlation strength parameter,  $q_{INV}$  is one dimensional momentum difference, defined as:

$$(3) \quad q_{INV} = \sqrt{|\mathbf{p}_1 - \mathbf{p}_2|^2 - (E_1 - E_2)^2}$$

where  $\mathbf{p}$  is the particle's momentum,  $E$  is the particle's energy.

Femtoscopy of photons, in contrast to hadrons, can reveal source's dynamics and geometry before its evolution stops (in other words, before kinetic freeze-out), thanks to previously mentioned penetrative nature of  $\gamma$  particles. Moreover, because femtoscopy is sensitive to the emission sequence of correlated particles, it can feasibly serve as a tool to differentiate photon contributions from various sources, allowing measurement of direct photons yield [5]. Additionally, since photons are mass-less, photon pair invariant mass is exactly equal to  $q_{INV}$ :

$$(4) \quad M_{\gamma\gamma} = \sqrt{2E_1 E_2 (1 - \cos \alpha_{\gamma\gamma})} = q_{INV}$$

where  $E$  is photon's energy,  $\alpha_{\gamma\gamma}$  is the opening angle between photons. Therefore a clear relation can be established between photon's energy, pair opening angle and  $q_{INV}$ ,

important from experimental point of view when choosing selection criteria, as well as for identification of residual correlations.

### 3. – HADES experiment

The HADES experiment [6], as a part of FAIR-GSI scientific complex [7], specializes in dilepton detection originating from light vector meson decays, such as  $\rho$  or  $\omega$ . It is designed to operate with beam kinetic energy of 1-2 A GeV, covering region of phase diagram corresponding to neutron stars and neutron star mergers. The HADES spectrometer [8] works in a fixed target mode, covering  $2\pi$  azimuthal angle and polar angle from  $18^\circ$  to  $88^\circ$ . It is capable of exceptional dilepton reconstruction efficiency,  $p\pi^\pm$  separation, as well as neutral particle reconstruction (thanks to electromagnetic calorimeters (ECAL) [9]).

### 4. – Photons at HADES

Because most detectors used in high-energy physics cannot detect neutral particles, photon reconstruction can be achieved either by utilising photon conversion method (PCM) [10] or with assistance of electromagnetic calorimeters.

Photon conversion method, due to HADES's specialization in dilepton reconstruction, provides excellent resolution and purity of obtained photon sample. Unfortunately, because it is an indirect detection method (requiring reconstruction  $e^\pm$  first and combining them into  $\gamma \rightarrow e^+e^-$  channel) it suffers from very low efficiency, reduced even further by low conversion probability in detector's material [11]. Consequently, it has been found unsuitable for conducting femtosopic measurements.

Electromagnetic calorimeters allow for the direct detection of neutral particles, thus provide noticeably higher efficiency than PCM, alongside wider transverse momentum and energy coverage. This is important from the point of view of direct photon reconstruction, since they are expected to occupy high  $p_T$  regions [4]. However, calorimeters suffer low granularity and energy resolution behaving like  $\sigma_E \sim \frac{1}{\sqrt{E}}$ , meaning correlation region ( $q_{INV} < 100$  MeV/c) can suffer from higher systematical uncertainty (see eq. (4)).

The photon sample with use of ECAL detector was selected by rejecting all hits correlated with charged tracks, along with minimum required energy of 100 MeV (to improve energy resolution and suppress neutron contamination) and  $\beta$  requirement ( $\pm 2\sigma$  from expected  $\beta = 1$  peak for every module separately). Figure 1 presents  $\beta$  distribution and number of reconstructed candidates per event for UrQMD [13] simulations with implemented detector response in GEANT [12] and experimental data for 0-40% centrality. The more spread distribution of  $\beta$  for the experiment compared to the simulation is caused by higher-than-expected noise in some of the ECAL modules.

### 5. – Photon-photon correlation functions

Before constructing correlation functions from obtained photon sample a two-particle detector effects need to be addressed.

For ECAL, due to the angular size of the modules, no photon pair can be reconstructed for an opening angle  $\alpha_{\gamma\gamma} < 4.4^\circ$ . Consequently, fewer pairs can contribute to the numerator of the correlation function than to the denominator (see eq. (1)), since mentioned limitation exists only within same event. Such effect is known as merging.

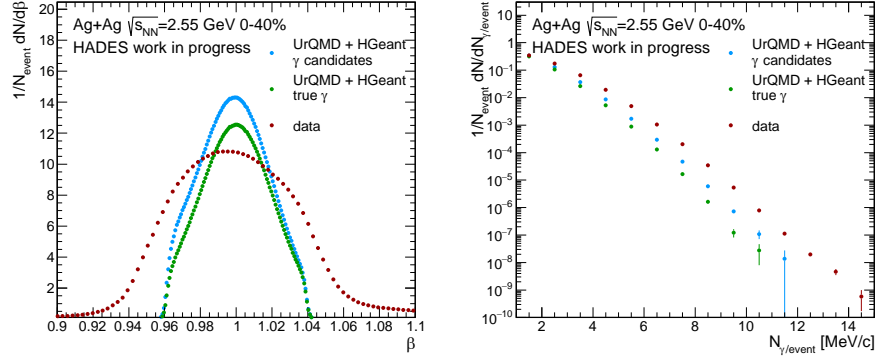


Fig. 1. – ECAL  $\beta$  (left) and photons per event (right) distributions. Blue circles represent all particles meeting selection criteria. Green show truly reconstructed  $\gamma$  particles with used approach. Red circles show selected particles from experimental data.

Moreover, because single photon can trigger more than one module, all ECAL towers triggered by same the particle are gathered in so-called clusters. Naturally, the  $\alpha_{\gamma\gamma}$  limitation should increase with increasing cluster size, as a single module cannot detect two photons in time window smaller than 500 ps [9]. However, it was found that despite such limits, some particles rarely exceed them. Simulation results suggest that this is most likely due to errors in the clusterization process, as in such cases both clusters were pointing at the same particle's track. Therefore one needs to not only apply  $\alpha_{\gamma\gamma}$  limitations to account for limited granularity, but also to suppress mentioned "cluster split" issue, simultaneously keeping limitations as low as possible due to  $q_{inv}$  -  $\alpha_{\gamma\gamma}$  relation (see eq. (4)). In order to do so, a distribution of the opening angle of "split clusters" was made with use of UrQMD + GEANT simulations, for every plausible size combination. Based on that, the minimum acceptable thresholds of  $\alpha_{\gamma\gamma}$  were established. Figure 2 shows thresholds map, along with example distribution of "split clusters"  $\alpha_{\gamma\gamma}$ .

Another effect worth concerning is sample purity. Such factor can be included by introducing purity correction to correlation function, defined as:

$$(5) \quad CF_{corr}(q_{INV}) = \frac{CF(q_{INV}) - 1}{purity(q_{INV})} + 1$$

where  $CF(q_{INV})$  is measured correlation function,  $purity(q_{INV})$  is purity function value, for the purpose of this analysis estimated from simulations and defined as:

$$(6) \quad purity(q_{INV}) = \frac{N_{\gamma\gamma}(q_{INV})}{N_{all}(q_{INV})}$$

where  $N_{\gamma\gamma}(q_{INV})$  is number of true photon pairs and  $N_{all}(q_{INV})$  is number of all accepted pairs for given  $q_{INV}$ . Figure 3 presents purity distribution as a function of  $q_{INV}$ .

Photon correlation functions, before and after merging and purity corrections, are shown in the fig. 4. For simulations, no femtoscopic effects are present. Accordingly,

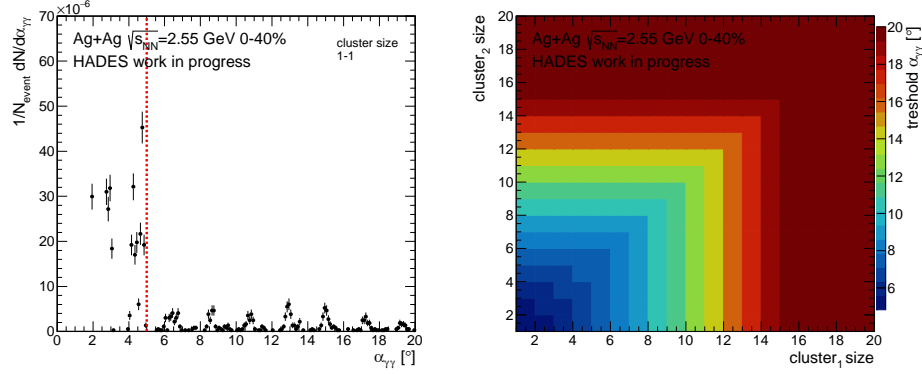


Fig. 2. – Distribution of  $\alpha_{\gamma\gamma}$  of "split clusters", both having size = 1 (left) and minimum threshold value in respect to cluster sizes of both photons (right). Dashed red line in the left fig. shows selected cutoff value.

respective correlation function is expected to be equal to unity, with the only exceptions being detector effects and residual correlations. Such residual correlation is clearly visible as Gaussian peak at  $q_{inv} \sim 135$  MeV/c, originating from  $\pi^0 \rightarrow \gamma\gamma$  channel. Additionally, before applying corrections a strong downwards trend is visible for both series. Comparing experimental results to the simulations after applying corrections reveals a clear enhancement in the experimental function at  $q_{INV} < 60$  MeV/c, reminiscent of the expected Bose-Einstein correlation, while simulated function remains around unity.

The experimental correlation function was fitted with modified parametrization described in eq. (2), featuring description of additional contribution:

$$(7) \quad CF(q_{INV}) = 1 + \lambda e^{-q_{INV}^2 R_{INV}^2} + \frac{a_0}{(1 + a_1 q_{INV})^{a_2}}$$

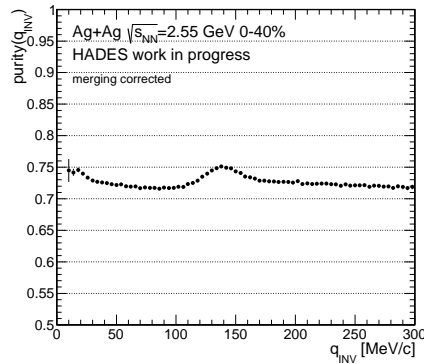


Fig. 3. – Photon pair purity in respect to  $q_{INV}$ . Estimated with use of UrQMD + GEANT simulations. Merging correction implemented.

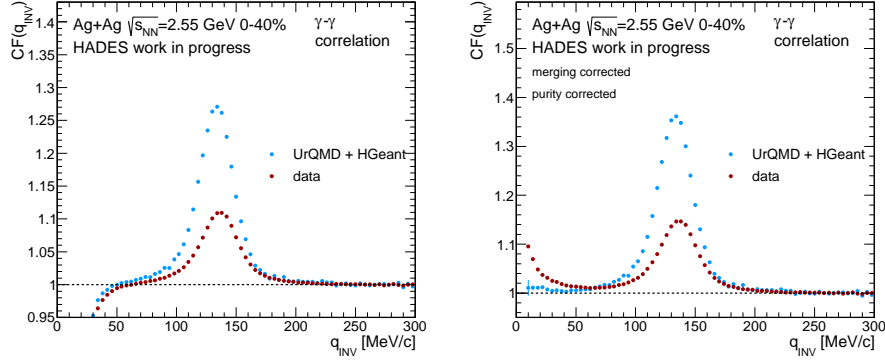


Fig. 4. – Photon-photon correlation function before (left) and after (right) necessary corrections. Blue circles represent UrQMD + GEANT simulations, red show experimental data.

where  $a_0, a_1, a_2$  are parameters for the background contribution. The result of fitting is shown in the fig. 5. First few points were excluded from fitting due to possible remains of detector effects.

To identify the origin of the additional contribution, SMASH [14,15] simulations were utilized, featuring only photons originating from  $\pi^0$  decays. Quantum statistics effect were implemented, along with estimated resolution of ECAL calorimeters. The addition of quantum statistics creates similar contribution to that visible in experimental results, regardless of detector resolution. Therefore it might be related to possible  $\pi^0 - \pi^0$

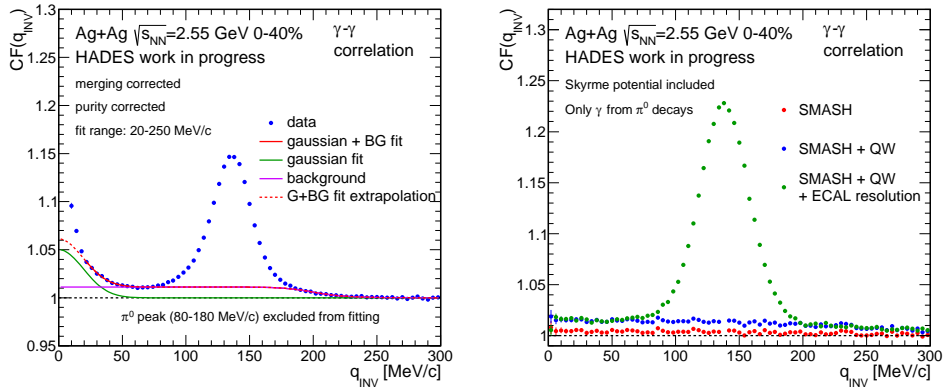


Fig. 5. – Experimental data correlation function fitted with parametrization (7) (left), photon-photon correlation function obtained with SMASH simulations (right). Red circles show "pure" SMASH output. Blue circles show addition of quantum statistics effects. Green circles feature additional detector resolution effects.

correlation contribution. It is also worth noticing that no enhancement at  $q_{INV} < 60$  MeV/c is visible in that case, suggesting no connection to  $\pi^0$  photons or being an artifact of detector's resolution. Hence, one may conjecture it as possible direct photon correlation. Further studies may provide better insight on such phenomenon.

## 6. – Summary

The photon-photon correlations can be achieved at the HADES experiment with use of electromagnetic calorimeters. The results show an enhancement at low  $q_{INV}$  region, most likely being a signature of expected Bose-Einstein correlation. Additional contribution was identified, with a plausible explanation of  $\pi^0 - \pi^0$  correlation signature. The qualitative description of correlation function was obtained with use of parametrization described by eq. (7), although in light of explanation of background contribution double Gaussian might be approached. The quantitative correlation function description is necessary, requiring systematical uncertainties estimation, as well as more detailed analysis of visible contributions. Future studies may provide the necessary information.

\* \* \*

This work was supported by the Grant of National Science Centre, Poland, No: 2020/38/E/ST2/00019. Studies were funded by IDUB-POB-FWEiTE-3, project granted by Warsaw University of Technology under the program Excellence Initiative: Research University (ID-UB).

## REFERENCES

- [1] GABOR D., *Rep. Prog. Phys.*, **83** (2020) 4.
- [2] LISA M. A., PRATT S., SOLTZ R. and WIEDEMANN U., *Annu. Rev. Nucl. Part. Sci.*, **55** (2005) 1.
- [3] HANBURY BROWN R. and TWISS R. Q., *London Edinburgh Philos. Mag. J. Sci.*, **45** (1954) 366.
- [4] BLAU D. and PERESUNKO D., *Particles*, **6** (2023) 1.
- [5] WA98 COLLABORATION (AGGARWAL M. M.), *Phys. Rev. Lett.*, **93** (2004) 2.
- [6] HADES webpage, <https://hades.gsi.de/>, accessed 08-01-2024.
- [7] GSI webpage, <https://www.gsi.de/en/start/news>, accessed 10-01-2024.
- [8] HADES COLLABORATION, *Eur. Phys. J. A*, **41** (2009) 2.
- [9] SVOBODA O. *et al.*, *JINST*, **9** (2014) 5.
- [10] POVAR T., *PoS, FAIRness2022* (2023) 047.
- [11] BEHNKE C., *J. Phys.: Conf. Ser.*, **503** (2014) 1.
- [12] BRUN R., BRUYANT F., MAIRE M., MCPHERSON A. C. and ZANARINI P., *GEANT 3: User's Guide Geant 3.10, Geant 3.11; rev. version*, <https://cds.cern.ch/record/1119728>, accessed 10-01-2024.
- [13] *Ultrarelativistic Quantum Molecular Dynamics*, <https://urqmd.org/>, accessed 10-01-2024.
- [14] PETERSEN H., OLINYCHENKO D., MAYER M., STAUDENMAIER J. and RYU S., *Nucl. Phys. A*, **982** (2019) 399.
- [15] SCHÄFER A. and ELFNER H., *SMASH - A Novel Transport Model to Simulate Low-Energy Hadronic Interactions*, [https://indico.scc.kit.edu/event/529/contribution/5482/attachments/2753/3955/SMASH\\_CORSIKA.pdf](https://indico.scc.kit.edu/event/529/contribution/5482/attachments/2753/3955/SMASH_CORSIKA.pdf), accessed 12-01-2024.